PHYSICAL REVIEW B, VOLUME 63, 161101(R)

Large birefringence in two-dimensional silicon photonic crystals

F. Genereux,* S. W. Leonard, and H. M. van Driel
Department of Physics, University of Toronto, 60 St. George Street, Toronto, Ontario M5S 1A7, Canada

A. Birner† and U. Gösele
Max-Planck-Institute of Microstructure Physics, Weinberg 2, D-06120 Halle, Germany

(Received 11 October 2000; published 3 April 2001)

We report an experimental and theoretical study of the birefringence of two-dimensional photonic crystals in the spectral region below the first photonic band gap. Transmission spectroscopy is used to measure the birefringence of a sample composed of a triangular lattice of air cylinders in silicon, with a cylinder radius of 0.644 μm and a lattice pitch of 1.5 μm. The measured birefringence (defined as the difference in the effective refractive indices of the electric fields polarized parallel and perpendicular to the cylinder axis) reaches a maximum value of 0.366 near the first photonic band edge at a wavelength of 6.52 μm. The results show excellent agreement with theory and demonstrate the potential use of two-dimensional photonic crystals for highly birefringent optically integrated devices.

DOI: 10.1103/PhysRevB.63.161101 PACS number(s): 42.70.Qs, 42.25.Lc, 42.79.−e

The ability to engineer photonic crystals using microstructured periodic dielectric materials has recently generated a great deal of interest from both a fundamental and an applied perspective. Much of this interest has been generated from the potential use of a photonic band gap to provide a new means of tailoring the emission and flow of light. However, photonic crystals, even those without a photonic band gap, possess many other interesting and practical properties related to the dispersion, anisotropy, and polarization characteristics of the photonic bands. For example, these properties of photonic crystals offer the opportunity to create low-threshold lasers,[1] efficient dispersion compensation,[2] enhanced nonlinear frequency conversion,[3,4] and novel superprism phenomena.[5]

Another property that is related to the polarization, anisotropy, and dispersion of photonic bands is birefringence (also known as double refraction). This property is clearly evident when the wavelength of light approaches the lattice constant, and the photonic bands become highly dispersive and sensitive to the direction of propagation. Recently, experiments in layered two-dimensional photonic crystals[6] and photonic crystal fibers of low symmetry[7] have demonstrated large birefringence[8] in this regime. However, many theoretical studies[9–12] have also shown that photonic crystals can possess large birefringence in the long-wavelength limit. Indeed, all two-dimensional photonic crystals share this interesting property.[11] It is expected that the ability to create a local, artificially birefringent medium on a dielectric chip will lead to many useful devices and applications for integrated optics.

In this paper, we present what we believe to be the first experimental study of photonic crystal birefringence within the first photonic band. Polarization-sensitive transmission spectroscopy is used to measure the birefringence of a two-dimensional photonic crystal composed of a triangular lattice of air cylinders in silicon. The results reveal a very large birefringence (defined as the difference in the effective refractive indices for the electric fields polarized parallel and perpendicular to the cylinder axis), with a maximum value of 0.366 near the first band gap. We also perform calculations of the birefringence using a plane-wave expansion method, and find excellent agreement with our measurements.

We fabricated two-dimensional photonic crystals using the techniques described in Refs. 13–16. Briefly, photolithography and alkaline etching were used to define a triangular lattice of pore nuclei, with a lattice constant of $a = 1.50$ μm, on a moderately *n*-doped silicon wafer. The patterned wafer was anodically etched in HF while being illuminated from the backside, forming cylindrical pores with a radius of $r = 0.45$ μm and a depth of 100 μm. The pore radius was subsequently widened via thermal oxidation and wet etching to 0.644 μm ($r/a = 0.429$). Using the method outlined in Ref. 17, the porous wafers were then microstructured into bars with well-defined surfaces for transmission experiments. A scanning electron microscope image of a thin microstructured bar (oriented in the Γ-*K* direction) is shown in Fig. 1. A wide sample of width 235.5 ± 1 μm (181 pore rows, oriented in the Γ-*M* direction) was prepared for this

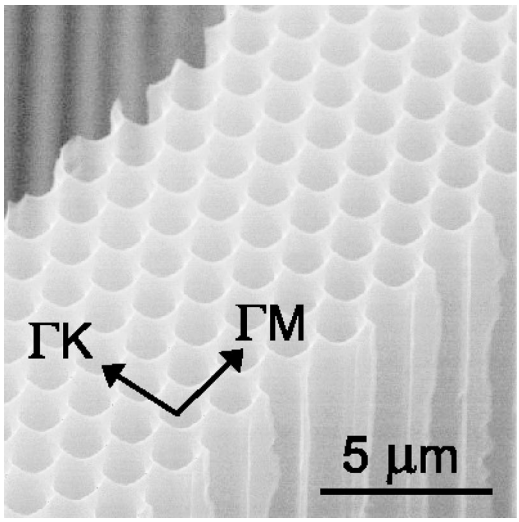

FIG. 1. Scanning electron microscope image of thin bar of macroporous silicon photonic crystal, oriented in the Γ-*K* direction.

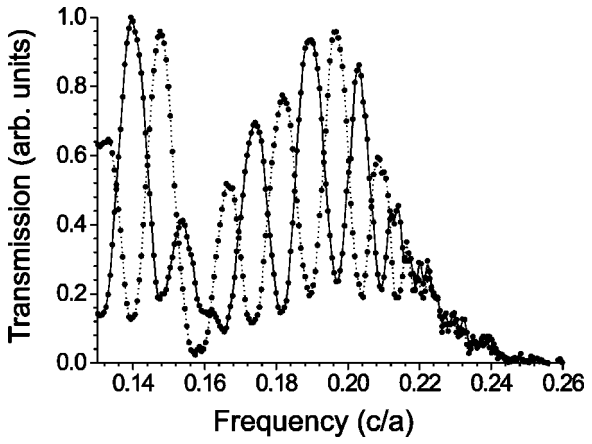

FIG. 2. Measured transmission spectra with parallel (solid) and perpendicular (dashed) polarizer orientations.

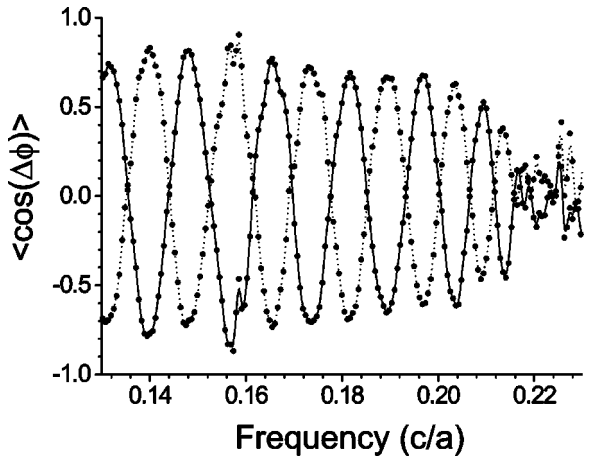

FIG. 3. Extracted cosine dependence from parallel (solid) and perpendicular (dashed) polarizer orientations.

experiment so that a large phase shift would occur between the *E*- and *H*-polarized beams upon transmission. The first photonic band edges for this sample occurred at $f_E = 0.230\ c/a$ (at a wavelength of $\lambda = 6.52\ \mu$m) and $f_H = 0.251\ c/a$ ($\lambda = 5.98\ \mu$m) for the *E*- and *H*-polarized fields,[18] respectively.

The photonic crystal birefringence was measured by placing the sample between a pair of polarizers and measuring the transmission spectrum with a Bomem Fourier transform infrared spectrometer equipped with a mercury cadmium telluride detector. The polarizer in front of the sample was oriented at an angle of 45° relative to the photonic crystal pore axis and the second polarizer was oriented either parallel or perpendicular to the first polarizer. Measurements were made over the wavelength range of 5.8–11.5 μm (i.e., over the frequency interval $0.13–0.26c/a$).

The measured transmission spectra for parallel and perpendicular polarizer orientations are shown in Fig. 2. The spectra show polarization beating indicative of a highly birefringent medium. The visibility of the peaks and the transmission amplitude decay as the frequency approaches that of the first photonic band edge at f_E. At frequencies between f_E and f_H, only the *H*-polarized beam is transmitted and interference cannot occur. The reduced transmission near the frequencies $f = 0.13$ and 0.16 is due to absorption in the natural SiO_2 layer coating the pores.

The oscillatory structure observed in Fig. 2 results from the interference of the *E*- and *H*-polarized beams when projected along a common polarization axis by the second polarizer. If multiple reflections are neglected and perfect coherence is assumed, the transmission spectra of the parallel and perpendicular polarizer orientations are given by

$$T(f) = \tfrac{1}{4}\{T_E(f) + T_H(f) \pm 2\sqrt{T_E(f)T_H(f)}\cos[\Delta\phi(f)]\}, \tag{1}$$

where $\Delta\phi = 2\pi\Delta n t f/c$ is the relative phase difference between the beams, Δn is the difference between *E*- and *H*-polarized refractive indices, T_E and T_H are the transmission coefficients of the *E*- and *H*-polarized fields, respectively, and t is the sample thickness. The sign of the final term is positive for the parallel orientation and negative for the perpendicular orientation. With the polarizers oriented at an angle of 45° relative to the photonic crystal pore axis, the interference will be complete only if the *E*- and *H*-polarized transmission coefficients are equal and the two fields are perfectly coherent (i.e., the two interferometric paths are balanced).

Our measured *E*- and *H*-polarized transmission spectra had different amplitudes, complicating the interpretation of the spectrum of Fig. 2 in terms of Eq. (1). We therefore inverted Eq. (1) using the measured *E*- and *H*-polarized transmission spectra (with both polarizers) to obtain the cosine function $\langle\cos(\Delta\phi)\rangle$. Here the brackets imply that the function involves a spatial average of the phase lag along the length of the sample due to local fluctuations in the sample thickness.

The resulting cosine dependence is shown in Fig. 3, illustrating the validity of Eq. (1). The observed dependence is well described by a cosine function multiplied by an envelope function that decreases as the first photonic band edge is approached. The fact that the envelope function is less than unity is related to the coherence properties of the optical source and the fluctuations in the sample width.[19]

The oscillations in Fig. 3 provide detailed information about the spectral dependence of Δn. For the case of parallel polarizers, a maximum implies that the phase delay is given by $\Delta\phi = 2\pi\Delta n t f/c = 2m\pi$, where m is a positive integer. A minimum implies that the phase delay is given by $(2m-1)\pi$. The reverse is true for the case of perpendicular polarizers. By measuring the frequency of each maximum and minimum and determining the corresponding value of m, we obtained the birefringence as a function of frequency. The result is shown in Fig. 4, where a large birefringence with a strong spectral dependence is observed. The maximum birefringence observed was $\Delta n = 0.366 \pm 0.002$ at a frequency of $f = 0.209 \pm 0.001 c/a$. This observed birefringence is very large compared to the birefringence typically found in naturally anisotropic crystals. For example, the maximum measured birefringence of our photonic crystal exceeds that of quartz[20,21] by a factor of 43.

In order to understand the nature of the observed dependence, we performed calculations of the photonic band struc-

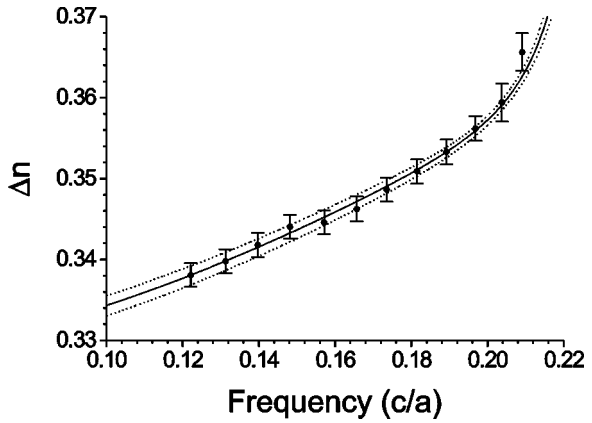

FIG. 4. Measured (data points) and calculated (curves) spectral dependence of effective birefringence. The dashed curves represent the calculated dependence for the upper and lower bounds of the measured value of r/a (0.429 ± 0.002).

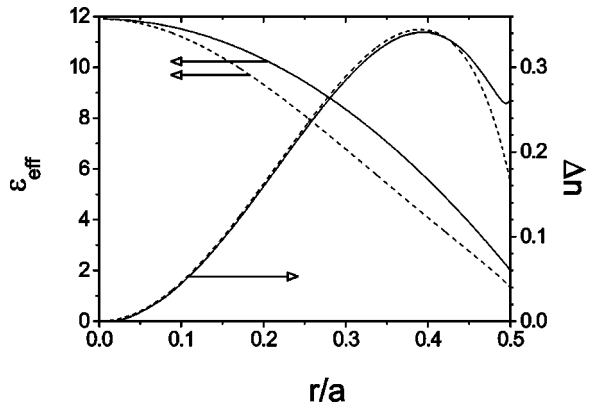

FIG. 5. Effective dielectric constants (ϵ_{eff}) and birefringence of two-dimensional photonic crystal of air cylinders in silicon. Left axis: effective dielectric constants of *E* (solid) and *H* (dashed) polarized fields. Right axis: effective birefringence of photonic crystal (solid) and associated random two-dimensional system (dashed).

ture using a plane-wave expansion method. Calculations were made using 500 plane waves and a dielectric constant of silicon of 11.7, and the resulting dispersion relation was used to obtain the effective refractive indices for the first photonic bands of the *E*- and *H*-polarized fields. We extended the long-wavelength effective index to the entire first photonic band with the definition $n_{\text{eff}} \equiv ck/\omega$, where k is the Bloch wave vector and c is the speed of light in vacuum. The resulting effective birefringence is also shown in Fig. 4, and agrees very well with the measured results. We therefore conclude that due to the increasing dispersion of the photonic bands with increasing frequency, the effective birefringence monotonically increases from its value in the long-wavelength limit.

We also used the plane-wave method of Kirchner *et al.*[10] to calculate the birefringence in the long-wavelength limit and its dependence on the cylinder radius. As a result of the scalar nature of the *E*-polarized field (electric field normal to periodic plane), the *E*-polarized effective dielectric constant in the long-wavelength limit is simply given by the spatial average of the two dielectric constants forming the composite. However, the *H*-polarized field is a vector field whose dielectric constant involves a complicated sum, with each term in the sum involving a product of three Fourier coefficients of the dielectric constant [see Eqs. (C12)–(C16) of Ref. 10]. We performed calculations using the same parameters as above and found that 400 plane waves provided sufficient convergence.

The calculated long-wavelength dependence of the effective dielectric constants and birefringence on the ratio of the pore radius to the lattice pitch (r/a) is shown in Fig. 5. The results illustrate that the two-dimensional photonic crystal acts as a highly birefringent positive uniaxial crystal in the long-wavelength limit, with the optic axis parallel to the pore axis. The birefringence spans a large range of values as the cylinder radius is varied and reaches a maximum value of 0.341 at a pore radius satisfying $r/a = 0.395$.

It is interesting to note that the long-wavelength photonic crystal birefringence can be reproduced with reasonable accuracy by calculations assuming a random medium in the long-wavelength limit.[10] Indeed, the *E*-polarized effective dielectric constant for a two-dimensional random medium is identical to that obtained for the periodic system. The *H*-polarized dielectric constant is well-approximated by the Maxwell-Garnet theory. The resulting random medium birefringence is also plotted in Fig. 5, and shows excellent agreement in the low-filling (i.e., small r/a) limit. The random medium birefringence only begins to show large departures from its periodic counterpart beyond $r/a \sim 0.4$, near the transition from an indirect to a direct system at $r/a = 0.5$ (where the adjacent pores begin to intersect and the Maxwell-Garnet theory fails). It is tempting to conclude from this result that the birefringence is not sensitive to the local order of the system (other than the volume fractions of the two dielectric constants). However, photonic crystals of lower symmetry are often biaxial[11] in the long-wavelength limit, revealing that the local structure of the system plays an important role in determining the long-wavelength optical properties. Furthermore, two-dimensional photonic crystals exhibit birefringence that increases with frequency within the first photonic band, without the drawback of the increased scattering that occurs in disordered systems.

Our results indicate that two-dimensional photonic crystals offer a new means of engineering highly birefringent materials on a micron scale. Photonic crystal birefringence could be used to create a wide array of photonic devices, including waveplates, polarization rotators, optical isolators and beamsplitters. Unlike conventional birefringent materials, these devices could be fabricated locally on an otherwise isotropic dielectric wafer and easily integrated with other devices. Although the calculated maximum long-wavelength birefringence of 0.341 is large compared to naturally anisotropic crystals, it can be further enhanced by using a photonic crystal with the direct topology (i.e., silicon cylinders). Indeed, a photonic crystal composed of a triangular lattice of silicon cylinders has a maximum long-wavelength birefringence of 0.938 (for a cylinder radius satisfying $r/a = 0.400$). The long-wavelength dependence of the principal dielectric constants of square and triangular photonic crystals, both direct and indirect, are shown in Fig. 1(b) of Ref.

12. The birefringence of the square crystal is similar to that of the triangular crystal (see Fig. 5) and is also largest for the indirect topology. We also note that it is possible to choose a topology with effective refractive indices close to that of glass, in which case the insertion loss from an optical fiber could be minimized.

In summary, we have demonstrated that two-dimensional photonic crystals act as highly birefringent media in the long-wavelength regime. We have measured the birefringence of two-dimensional silicon photonic crystals within the first photonic band via transmission spectroscopy. The results, which showed a very large birefringence that agreed very well with theory, highlight the potential use of photonic crystal birefringent elements for integrated optics applications.

We thank Kurt Busch for useful suggestions. Three of the authors (S.W.L., H.V.D., and F.G.) gratefully acknowledge the financial support of the Natural Sciences and Engineering Research Council of Canada and Photonics Research Ontario.

---

*Present address: COPL, Dept. Génie électrique, Pavillon Adrien Pouliot, Université Laval, Ste-Foy, Quebec G1K 7P4, Canada.

†Present address: Infineon Technologies AG, Königsbrücker Strasse 180, D-01099 Dresden, Germany.

[1] J. P. Dowling, M. Scalora, M. J. Bloemer, and C. M. Bowden, J. Appl. Phys. **75**, 1896 (1994).

[2] T. A. Birks, D. Mogilevtsev, J. C. Knight, and P. St. J. Russell, IEEE Photonics Technol. Lett. **11**, 674 (1999).

[3] V. Berger, Phys. Rev. Lett. **81**, 4136 (1998).

[4] N. Bloembergen and A. J. Sievers, Appl. Phys. Lett. **17**, 483 (1970).

[5] H. Kosaka, T. Kawashima, A. Tomita, M. Notomi, T. Tamamura, T. Sato, and S. Kawakami, Phys. Rev. B **58**, R10 096 (1998).

[6] T. Sato, K. Miura, Y. Ohtear, S. Kawakami, and T. Tamamura, QELS 2000 Technical Digest, Conference Edition (Optical Society of America, Washington, D.C., 2000), p. 73.

[7] A. Ortigosa-Blanch, J. C. Knight, W. J. Wadsworth, J. Arriaga, B. J. Mangan, T. A. Birks, and P. St. J. Russell, Opt. Lett. **25**, 1325 (2000).

[8] The birefringence values, defined by the difference in the refractive indices of the two polarizations, were 0.19 and 3.7×10^{-3} for Refs. 6 and 7, respectively.

[9] S. Datta, C. T. Chan, K. M. Ho, and C. M. Soukoulis, Phys. Rev. B **48**, 14 936 (1993).

[10] A. Kirchner, K. Busch, and C. M. Soukoulis, Phys. Rev. B **57**, 277 (1998).

[11] P. Halevi, A. A. Krokhin, and J. Arriaga, Appl. Phys. Lett. **75**, 2725 (1999).

[12] P. Halevi, A. A. Krokhin, and J. Arriaga, Phys. Rev. Lett. **82**, 719 (1999).

[13] U. Grüning, V. Lehmann, S. Ottow, and K. Busch, Appl. Phys. Lett. **68**, 747 (1996).

[14] A. Birner, U. Grüning, S. Ottow, A. Schneider, F. Müller, V. Lehmann, H. Föll, and U. Gösele, Phys Status Solidi A **165**, 111 (1998).

[15] V. Lehmann, J. Electrochem. Soc. **140**, 2836 (1993).

[16] S. Rönnebeck, J. Carstensen, S. Ottow, and H. Föll, Electrochem. Solid-State Lett. **2**, 126 (1999).

[17] S. Ottow, V. Lehmann, and H. Föll, J. Electrochem. Soc. **143**, 385 (1996).

[18] The *E*- and *H*-polarized electric fields are parallel to the cylinder axis and in the periodic plane of the crystal, respectively.

[19] The *E*- and *H*-polarized fields were partially coherent and could not completely interfere to give a cosine of unit amplitude in the long wavelength limit. The free-space coherence length of the source was 1.25 mm, which was reduced by roughly a factor of 2 inside the sample. The long sample width of 235.5 μm thus prohibits the multiple reflections from properly interfering, washing out the Fábry-Perot oscillations in transmission. More importantly, fluctuations in the sample width cause the phase lag $\Delta\phi(f)$ to vary across the length of the sample, and the sensitivity to this effect increases dramatically as the band edge is approached.

[20] The birefringence of quartz is 8.5×10^{-3} at a wavelength of 1.5 μm (Ref. 21).

[21] H. R. Philipp, in *Handbook of Optical Constants of Solids*, edited by E. Palik (Academic Press Inc., Florida, 1985), p. 729.